



# HHS Public Access

Author manuscript

*ACS Appl Bio Mater.* Author manuscript; available in PMC 2022 November 22.

Published in final edited form as:

*ACS Appl Bio Mater.* 2020 November 16; 3(11): 7677–7686. doi:10.1021/acsabm.0c00862.

## Electrospun Bioabsorbable Fibers Containing S-Nitrosoglutathione for Tissue Engineering Applications

**Sean P. Hopkins,**

School of Chemical, Materials and Biomedical Engineering, University of Georgia, Athens 30602, Georgia, United States

**Jitendra Pant,**

School of Chemical, Materials and Biomedical Engineering, University of Georgia, Athens 30602, Georgia, United States

**Marcus J. Goudie,**

School of Chemical, Materials and Biomedical Engineering, University of Georgia, Athens 30602, Georgia, United States

**Dieu Thao Nguyen,**

School of Chemical, Materials and Biomedical Engineering, University of Georgia, Athens 30602, Georgia, United States

**Hitesh Handa**

School of Chemical, Materials and Biomedical Engineering, University of Georgia, Athens 30602, Georgia, United States

### Abstract

Blended and coaxial fibers comprising polycaprolactone and gelatin, containing the endogenous nitric oxide (NO) donor *S*-nitrosoglutathione (GSNO), were electrospun. Both types of fibers had their NO release profiles tested under physiological conditions to examine their potential applications as biomedical scaffolds. The coaxial fibers exhibited a prolonged and consistent release of NO over the course of 4 d from the core-encapsulated GSNO, while the blended fibers had a large initial release and leaching of GSNO that was exhausted over a shorter period of time. Bacterial testing of both fiber scaffolds was conducted over a 24 h period against *Staphylococcus aureus* (*S. aureus*) and demonstrated a 3-log reduction in bacterial viability. In addition, no cytotoxic response was reported when the material was tested on mouse fibroblast cells *in vitro*. These fibrous matrices were also shown to support cell growth, attachment, and overall activity of fibroblasts when exposed to NO, especially when GSNO was encapsulated within coaxial fibers. From an application point of view, these NO-releasing fibers offer great potential in tissue engineering and biomedical applications because of the crucial role of NO in

---

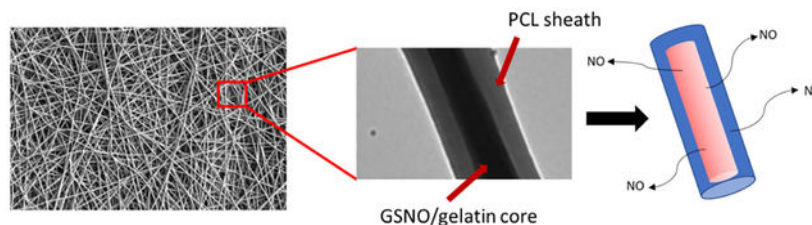
**Corresponding Author: Hitesh Handa** – School of Chemical, Materials and Biomedical Engineering, University of Georgia, Athens 30602, Georgia, United States; Phone: (706) 542-8109; hhanda@uga.edu.

Complete contact information is available at: <https://pubs.acs.org/10.1021/acsabm.0c00862>

The authors declare the following competing financial interest(s): Drs Hopkins and Handa work with a startup company in NOVeta Biomedical LLC exploring possibilities of using nitric oxide-releasing materials for medical applications.

regulating a variety of biological processes in humans such as angiogenesis, tissue remodeling, and eliminating foreign pathogens.

## Graphical Abstract



## Keywords

electrospun fibers; nitric oxide; infection; S-nitrosoglutathione; wound healing; cell scaffold

## 1. INTRODUCTION

The ongoing development of polymeric scaffolds used for cell support has vast potential as the area of tissue engineering continues to expand. By varying the types of polymers being used along with the method of processing the scaffold itself, these types of fabricated materials demonstrate a wide array of applications ranging from wound healing to bone tissue regeneration. A common characteristic that is important when developing these types of polymeric cell scaffolds is their ability to promote cell migration in order to successfully and quickly integrate the material into its surroundings. Highly porous structures, such as meshes, fibers, and sponges, are excellent at promoting this as they allow for a more uniform cell distribution across the structure while allowing for efficient diffusion of nutrients for the attached cells as well.<sup>1</sup>

A popular method to produce micro- and nanoscale fibers to form these types of scaffolds is electrospinning, where a polymer solution is subjected to a high voltage while simultaneously being ejected at a consistent rate via a syringe pump. The polymer ejected using this method is collected on a grounded target in the form of a fibrous mat. Either aligned or randomly directed fibers can be fabricated depending on the target being used. Rotating drums and mandrels are often used to ensure that the fibers are in the same direction, while stationary plates will collect fibers with no alignment. The scaffolds and meshes prepared through electrospinning have a variety of applications in fields related to tissue engineering, wound dressings, angiogenesis, and artificial bone scaffolds.<sup>2-5</sup> Because of the porosity and high surface area of electrospun scaffolds, they make excellent artificial extracellular matrices (ECMs) for cells, allowing for efficient cell migration, attachment, and proliferation. Electrospun scaffolds also have excellent versatility when adjusting their physical properties, as a variety of polymers can be used depending on the appropriate tissue application. The most common ECM component in the body is collagen, where fibril bundles vary in diameter from 50 to 500 nm, a size that can easily be produced through electrospinning.<sup>6</sup> This makes the electrospinning of polymers an ideal solution for fabricating a scaffold that is able to mimic common cellular interactions that occur within

the body. A common strategy to improve the efficacy of these fibrous scaffolds is through the addition of therapeutic components such as growth factors, antibiotics, and cancer treatments.<sup>7–10</sup>

Nitric oxide (NO)-releasing molecules are ideal to incorporate into polymeric biomaterials that are used for wound healing and other scaffold-related biomedical applications. This is due to the fact that NO can act as both an antibacterial agent and as a method to increase angiogenesis and collagen deposition to a desired implant site.<sup>11–13</sup> Reducing the overall bacterial burden of a wound is imperative to improve the efficacy and speed at which the wound healing process is resolved. The use of NO as a strategy to eliminate even troublesome antibiotic-resistant bacteria has become popular over the past several years.<sup>14–17</sup> This is due to the ability of NO to diffuse across bacterial membranes and cause direct nitrosative and oxidative damage. Another important antimicrobial mechanism seen with NO is its ability to disperse and prevent the formation of biofilms, which are highly resistant bacteria encapsulated within a protective polysaccharide matrix that prevents effective penetration of antibiotics.<sup>18,19</sup> Even low levels of NO have been shown to be able to disperse biofilms into a planktonic state, making them more vulnerable to traditional antibiotic treatments.<sup>20</sup> In wounds where chronic infections are common, the use of NO as a potential topical agent is able to address these complications.

The uses of NO-releasing fibers can be utilized in a variety of different types of tissue scaffolds because of its ability to upregulate certain cytokines and growth factors of certain cells. Exogenous delivery of NO has proven to increase the production of vascular endothelial growth factor (VEGF) from endothelial cells which as a result can shorten re-endothelialization time for artificial vascular grafts.<sup>21–23</sup> Consequentially, this will then promote vasculogenesis and angiogenesis, which greatly benefits implanted scaffolds through significantly increasing the rate at which the graft integrates into the surrounding tissue. Several types of electrospun fibers have been fabricated with different types of blended NO donors ranging from nanoparticles containing covalent bound diazeniumdiolates (NONOates) to *S*-nitrosothiols (RSNOs) physically blended within the polymer matrix.<sup>24,25</sup> The limitation with these types of blended fibers is their short-lived NO lifespan and high initial burst release, which can be unfavorable in certain biological environments. However, for short-term applications, this can be an effective strategy to obtain high bactericidal levels, while still providing a platform for cell migration and proliferation once the NO release is exhausted. A strategy to help slow NO release is through the use of coaxial electrospinning, where the NO donor is encapsulated within a protective polymer sheath. In the past, this approach has been used with synthetic NONOate-based donors, where polyamidoamine dendrimers were functionalized and then encapsulated within polyurethane composite fibers.<sup>26</sup> This method allowed for sustained release for up to 24 h and demonstrated potent antimicrobial capabilities. Because of this encapsulation, the high burst effect commonly seen with NONOates was lowered, which in turn lowered the potential cytotoxic effects toward mouse fibroblast cells.

In the current study, the NO-releasing characteristics and physical properties of blended and coaxial electrospun fibers were investigated and compared using bioabsorbable polymers in conjunction with an endogenous RSNO, *S*-nitrosoglutathione (GSNO). The comparison of

utilizing either a blended or coaxial strategy for incorporating NO was assessed to observe the potential distinct NO release trends from both types and how these specific trends impact their biocompatibility. For coaxial fibers, polycaprolactone (PCL) was used to electrospin the outer sheath, while gelatin-containing GSNO was used as the inner core fiber. Blended fibers containing the same polymer and GSNO ratios were fabricated to demonstrate the effectiveness of the PCL sheath in significantly increasing the NO release longevity of the coaxial fibers. The combination of PCL and gelatin was used specifically because of the biodegradability of the polymers along with their excellent biocompatible properties. The antimicrobial potential and cytotoxic effects of both types of fibers were examined to demonstrate that the NO release from the incorporated GSNO is effective against bacteria without causing any detrimental effect. These scaffolds were then directly used in cell culture to observe the affinity of fibroblasts to attach and proliferate in the presence of this exogenous delivery of NO.

## 2. EXPERIMENTAL SECTION

### 2.1. Materials.

Autoclaved phosphate-buffered saline (1× PBS) was used for all *in vitro* experiments. PCL ( $M_n = 80,000$ ), gelatin from bovine skin, DAPI, hydrochloric acid, sodium nitrite, copper(II) chloride, L-ascorbic acid sodium salt, acetone, Cell Counting Kit-8 (CCK-8), and 1,1,1,3,3,3-hexafluoroisopropanol (HFIP) were purchased from Sigma-Aldrich (St. Louis, MO). L-Glutathione (reduced 98+%) was obtained from Alfa Aesar (Ward Hill, MA). Alexa Fluor 488 Phalloidin was purchased from Thermo Fisher Scientific (Waltham, MA). Dulbecco's modified Eagle's medium (DMEM) and trypsin-EDTA were purchased from Corning (Manassas, VA). The antibiotic penicillin-streptomycin (Pen-Strep) and fetal bovine serum were purchased from Gibco-Life Technologies (Grand Island NY 14072). The mouse fibroblast cell line (ATCC 1658) and *Staphylococcus aureus* (ATCC 5538) were originally obtained from American Tissue Culture Collection (ATCC).

### 2.2. Synthesis of S-Nitrosoglutathione.

Synthesis of GSNO was carried out by following a slightly modified protocol developed by T.W. Hart.<sup>27</sup> First, glutathione (2.93 mmol, 900 mg) is dissolved in 4 mL of deionized water and 1.25 mL of 2 M HCl. The solution is allowed to chill in an ice bath for 10 min before a slight excess (3 mmol, 207 mg) of sodium nitrite is added, forming a dark red solution. This solution is further chilled for an additional 40 min. Although still in the ice bath, 5 mL of acetone is added to the solution and stirred for 10 min. The pink precipitate that forms is filtered out and washed with cold deionized water and acetone before being dried under vacuum overnight.

### 2.3. Fiber Fabrication.

To develop coaxial electrospun fibers, separate 10 mL plastic syringes containing either PCL or gelatin with 20 wt % GSNO were placed onto separate syringe pumps (Razel Scientific Instruments, St. Albans, VT) and fitted to a custom-built coaxial needle (Raméhart Instrument Co., Succasunna, NJ) (Figure 1). Before blending the GSNO into the gelatin, it was first pulverized into a fine powder using a mortar and pestle to ensure a more even

distribution through the solution and to prevent any larger particles from clogging in the needle during electrospinning. Solutions of gelatin and PCL were dissolved in HFIP at 10 wt %, which were chosen because of previous electrospinning optimization studies.<sup>28</sup> The gelatin–GSNO-containing syringe was attached to the inner portion of the needle (ID = 0.413 mm), while the PCL-filled syringe was attached as the outer sheath (ID = 0.838 mm). A high voltage power supply (Gamma High Voltage, Ormond Beach, FL) was used to supply 10.5 kV between the needle and the grounded collector which was positioned horizontally from the syringe pumps. The collector was made from aluminum foil and placed 10 cm away from the tip of the needle. The flow rate for the gelatin–GSNO solution was maintained at 0.56 mL h<sup>-1</sup>, and the PCL solution was at 0.70 mL h<sup>-1</sup>. After collection, the coaxial fiber mats were dried under vacuum at room temperature overnight. Blended fibers followed a similar procedure, but the two solutions are mixed together in a 1:1 ratio in a single syringe fitted with a needle (ID = 0.838 mm) at a flow rate of 1.13 mL h<sup>-1</sup>. The ratio at which the polymers were blended matched the composition seen in the coaxial fibers along with the final GSNO concentration.

#### 2.4. NO Release Measurements.

Real-time NO release from the fibrous matrices was measured through chemiluminescence using a Sievers nitric oxide analyzer (NOA), model 280i (Boulder, CO). The fibrous scaffolds were tested for passive NO release by submerging them into 0.01 M PBS containing EDTA at 37 °C inside of an amber reaction chamber. Nitrogen gas was then bubbled through the solution at a flow rate of 200 mL min<sup>-1</sup> to carry any NO being emitted to the NOA. Quantification of GSNO loading into the fibers was carried out by catalytically cleaving the S–N bond through the use of copper(II) chloride and ascorbic acid. Subsequent injections of copper solution are added until all the NO release was exhausted from the material.

#### 2.5. Characterization of GSNO-Containing Electrospun Fibers.

Fiber morphology for both types of fibers was observed using an FEI Teneo field emission scanning electron microscope (Hillsboro, OR). Coaxial fiber inner diameters were measured using an FEI Tecnaï 20 (FEI Co., Eindhoven Netherlands). Diameter and percent porosity were measured from SEM images using NIH ImageJ software (Bethesda, MD).

#### 2.6. Leaching Assay.

Leaching of GSNO from both blended and coaxial electrospun fibers was quantified using UV–vis spectroscopy and was each tested in triplicate. Samples were initially weighed and then submerged under a known volume of PBS at 37 °C. After 24 h, absorbance was measured at the GSNO's characteristic *S*-nitrosothiol peak in the UV region at 340 nm.<sup>27</sup>

#### 2.7. Quantification of Viable Bacterial Cells on Fibrous Surfaces.

A standard bacterial adhesion test was used to measure and compare the viability of adhered bacteria on the surface of the fibrous matrices.<sup>29,30</sup> *S. aureus*, one of the most common causal agents for biofilm formation and nosocomial infection, was used in the study as a proof of concept. A single colony of *S. aureus* was incubated in LB broth overnight, and

optical density at 600 nm was measured ( $OD_{600}$ ) using a UV-vis spectrophotometer. The bacteria were then washed twice with sterile PBS (pH 7.4) followed by centrifugation at 2500 rpm for 8 min. The fibers of each type and their respective control (without GSNO) were exposed for 24 h at 37 °C in triplicate to the bacterial culture, which was maintained at  $10^8$ – $10^{10}$  colony forming units (cfu) per mL. After 24 h, the fibrous sheets were rinsed gently to remove any loosely adhered bacteria and transferred to a fresh 2 mL sterile PBS solution. The material was then sonicated for 45 s using an Omni-Tip homogenizer to detach the adhered bacteria into the solution. The bacteria detached from the fibrous mats were then collected, serially diluted ( $10^{-1}$  to  $10^{-5}$ ), and plated in premade agar Petri dishes at a concentration of 20 g L<sup>-1</sup> of LB agar. After 20 h of incubation at 37 °C, the cfu's were counted and inhibition of attached bacteria was calculated using the formula below.

$$\% \text{ Bacterial inhibition} = \frac{\left( \frac{\text{cfu}}{\text{cm}^2} \text{ in control samples} - \frac{\text{cfu}}{\text{cm}^2} \text{ in test samples} \right) \times 100}{\frac{\text{cfu}}{\text{cm}^2} \text{ in control samples}}$$

## 2.8. *In Vitro* Cellular Response.

In the current study, using a protocol developed by Pant et al., the leachates were collected by soaking both types of fibrous mats containing GSNO in DMEM for 24 h followed by exposing the media to cultured mouse fibroblast cells.<sup>29</sup> Briefly, the cell culture of the mouse fibroblast cells was carried out by seeding cells in a 75 cm<sup>2</sup> T-flask and incubating them for approximately a week in a CO<sub>2</sub> incubator at 37 °C until the cells became 80–90% confluent. The cell culture media (DMEM) were changed intermittently every second day. Thereafter, cells were seeded (5000 cells mL<sup>-1</sup>) in a 96-well plate by first detaching them from the T-flask using trypsin–EDTA (0.18% trypsin with 5 mM EDTA) and allowed to incubate for another 24 h. After 24 h, when the cells formed a monolayer with the well plate, 10 μL of the respective leachate solution was added to the cells and exposed for a further 24 h. WST-8 dye-based standard cell cytotoxicity kit (CCK-8, Sigma-Aldrich) solution (10 μL) was then added to quantify the viability of the cells in the presence of leachates from control and NO-releasing fibers. The WST-8 forms an orange color product, formazan, on reacting with NADH from the living cells only, which was measured at 450 nm using a spectrophotometer microplate reader. The relative cell viability was measured using the formula below.

$$\text{Relative cell viability (\%)} = \frac{\text{absorbance of the test samples}}{\text{absorbance of the control samples}} \times 100$$

The cells obtained after trypsinization were also used to observe how both blended and coaxial NO-releasing fibers are able to support cell growth. In a six-well plate, fibrous mats were kept and then sterilized through UV exposure for 30 min. Thereafter, cell cultures containing 5000 cells mL<sup>-1</sup> were seeded on top of the electrospun fibers and allowed to attach and grow on the surface by placing the plate in the CO<sub>2</sub> incubator at 37 °C for 24 h. The cells were then stained with 4',6-diamidino-2-phenylindole (DAPI) to observe cell nuclei, while the cytoskeletal structure was visualized with Alexa Fluor 488 Phalloidin.

Briefly, the cells within the fibrous scaffolds were first fixed in 0.01 M PBS containing 5% paraformaldehyde. A dilution of 1:500 of phalloidin in PBS was then administered for 20 min followed by DAPI (300 nM in PBS) for 3 min. Finally, the overall cell growth and attachment were observed under a fluorescent microscope (EVOS XL, Thermo Fisher Scientific, Waltham, MA).

## 2.9. Statistical Analysis.

Data obtained were expressed as mean  $\pm$  standard deviation. Statistical analysis was carried out using a Student's *t*-test with SAS JMP software. The P value  $<0.05$  was considered statistically significant for all experiments throughout the study.

## 3. RESULTS AND DISCUSSION

### 3.1. Electrospinning of Blended and Coaxial Fibers Containing S-Nitrosoglutathione.

The utilization of fibers for producing environments to mimic the ECM in various parts of the body has been successfully used in areas such as artificial vascular grafts, bone scaffolds, platforms for stem cell differentiation, and wound healing patches.<sup>31–36</sup> Nanofiber-based scaffolds are a much more preferred structure for biomedical applications as they encourage cell attachment, proliferation, and directed migration.<sup>37–39</sup> By incorporating an endogenous NO donor such as GSNO into a fibrous platform, these beneficial properties become even more effective as NO has been shown to promote angiogenesis, act as a potent antimicrobial molecule, and reduce the overall foreign body response to blood and tissue contacting materials.<sup>40–43</sup> Specifically, this combination of NO release from a fibrous scaffold would be the most beneficial as a wound healing patch or scaffold.

The two polymers being utilized for the proposed fibrous scaffolds are PCL and gelatin. Composite fibers containing these two polymers have been previously fabricated into scaffolds as a method for neuronal regeneration, skin grafts, and promoting osteogenic differentiation of stem cells.<sup>44–46</sup> The combination of these two polymers have displayed excellent properties for cell attachment and ECM mimicry. The fibers that were fabricated in this study utilized this polymer combination in different ways, while incorporating GSNO as the endogenous NO donor in both blended and coaxial systems. Solutions were fabricated and adjusted to contain 10 wt % GSNO for the output electrospun fibers.

Blended fibers formed from different combinations of synthetic and natural polymers have been fabricated because of the complementary traits they possess.<sup>47–49</sup> Although natural polymers often have weak mechanical strength and high hydrophilicity as a standalone material, they possess excellent biocompatible properties and have been shown to promote cell adhesion, proliferation, migration, and differentiation when electrospun as nanofibers.<sup>50</sup> For polymer blends containing gelatin specifically, the fibrous mat becomes more porous as time passes because of its quick rate of degradation. For wound healing applications, this is a beneficial quality as it will allow more cell migration into the scaffold.

Coaxial fibers, specifically, have been used for scaffolds that deliver precise amounts of a drug or protein to the surrounding environment. Electrospinning of PCL–gelatin coaxial fibers has been previously reported as a controlled drug delivery system.<sup>51,52</sup> The fabricated

GSNO fibers are able to utilize the PCL layer as a protective sheath to maintain structural integrity, while preventing large burst releases of NO from the fibrous scaffolds. This allows for a consistent, leveled flux of NO to be maintained over a prolonged period of time, while blending the GSNO within the polymer matrix demonstrates a large burst release which can potentially be cytotoxic and significantly limit the release life of the material. An often primary reason why researchers will use a coaxial system as the target therapeutic molecule to be released is that it can be more controllable as it is protected from its surrounding biological environment.<sup>53</sup> The use of GSNO is an ideal molecule in this case as NO is a small molecule that is permeable through the PCL sheath, while the GSNO molecule itself is protected. The electrospinning setup for the fabrication of coaxial fibers is shown in Figure 1.

### 3.2. NO Release from Blended and Coaxial Electrospun Fiber Mats.

Blended and coaxial electrospun fibers containing GSNO were tested for NO release in real time using chemiluminescence. The total NO release was monitored until the fibrous mats were exhausted, and their flux measurements on each day are shown in Figure 2. Even though the GSNO content within both fiber types is identical, each composition gives a distinct NO-releasing profile because of the nature of how the NO donor is dispersed within the fibers. When blended, a large initial burst of NO ( $3.91 \pm 0.96 \times 10^{-10} \text{ mol mg}^{-1} \text{ min}^{-1}$ ) was seen, which then quickly dropped to the recorded flux (approximately  $0.21 \pm 0.14 \times 10^{-10} \text{ mol mg}^{-1} \text{ min}^{-1}$ ) over a 4 h period. Coaxially sheathed fibers demonstrated a low initial flux that slowly crept to a higher leveled release in comparison as the gelatin–GSNO core is dissolved. This higher sustained release is due to the slower rate at which the fibers ramp up to the final flux from the encapsulation effect that the PCL sheath provides. The largest difference in NO release was observed within the first 24 h of testing, while the following days showed no significant difference. Coaxial fibers were able to demonstrate a more prolonged release after this 24 h timepoint, which in turn may be the more preferential delivery of NO from a fibrous scaffold. Depending on the required application, either blended or coaxial electrospun fibers may be the more preferred method of NO delivery. Situations that require high levels of NO over a short period of time (<4 h) would benefit from using blended fibers, where the GSNO component can be allowed to leach out into the surrounding environment, while certain long-term, controlled applications would prefer the coaxial delivery of NO. In terms of biodegradable fibers, the sustained release demonstrated from the coaxial GSNO fibers exceed currently published NO-releasing fiber technology. Other NO fiber strategies tend to utilize NO-releasing particles that have a low total NO capacity or diazeniumdiolates molecules that release a majority of their NO within the first few hours, limiting their long-term potential.<sup>24,26</sup> In terms of total NO release, the fibers surpass the previously mentioned NO-releasing fiber strategies because of the large reservoir of GSNO we are able to compact within the core.

Wound healing would be an ideal example application for these types of GSNO-containing fibers as the sustained NO release can help facilitate angiogenesis and VEGF production, while acting as an antimicrobial agent simultaneously.<sup>54</sup> Direct delivery of GSNO as a NO carrier specifically has shown many beneficial effects in topical applications, allowing blended GSNO fibers, specifically, to have the potential to act as a localized GSNO delivery



vessel.<sup>55,56</sup> Because GSNO is an endogenous NO donor, direct delivery of low amounts of GSNO into surrounding tissue has been demonstrated in past studies to have no localized or systemic detrimental effects.<sup>57</sup>

For situations where a longer, steady level of NO release is required, it would be more beneficial to use coaxial fibers where the NO donor is dispersed within the inner gelatin core, while being encapsulated by the hydrophobic, degradable PCL sheath. This release can be further tuned using different outer sheath polymers with varying degradation rates and degrees of hydrophilicity. However, if certain hydrophilic polymers such as chitosan or alginate are used as shell polymers, extra cross-linking steps would need to be carried out to ensure that the fibers do not completely disassociate when placed under aqueous conditions. The blended GSNO composition could also be tuned in a similar manner but will most likely still exhaust a majority of its NO within the first 4 h simply because of the high surface area in combination with the hydrophilic properties of GSNO. Prolonging the longevity of the NO release kinetics or any type of drug release from fibrous polymers will revolve around using a coaxial strategy to ensure a more controlled release rate.

### 3.3. Physical Properties of Fibrous Matrices.

As shown in the SEM images in Figure 3, there is an observable difference between the blended and coaxial electrospun fibrous mats. Particles of GSNO are clearly visible on the surface of the fibers when the polymer solutions are blended together with GSNO, while the coaxial fibers had virtually none. This accounts for the higher initial NO release seen in the blended fibers which was shown earlier. The SEM images were also used to obtain the diameter distribution of the fibers, and it was calculated using ImageJ software (Figure 4). The blended fibers displayed a much wider variation of fiber diameters ( $781.4 \pm 528.4$  nm) compared to coaxial fibers ( $779.5 \pm 279.4$  nm). This could be due to the disruption the GSNO particles suspended within the polymer blend, causing irregularities as the polymer solution is ejected from the needle tip. More consistent fibers were clearly observed from the coaxial fibers as the GSNO is encapsulated within the inner needle during the electrospinning process.

The presence of high porosity within a polymer scaffold has been proven to accelerate tissue integration and remodeling.<sup>58,59</sup> In a fibrous system, the pores that are formed are due to the layer-by-layer deposition of fibers loosely overlapping with each other, compared to the fabrication of other porous materials that require the use of porogens or gas bubbles. The percent porosity was  $47.0 \pm 2.09\%$  for blended fibers, while coaxial fiber porosity was found to be  $50.9 \pm 4.76\%$ . Over time, the blended fibers will exhibit a more dynamic porosity when placed under physiological conditions because of the solubility and quick degradation of the gelatin portion. PCL–gelatin fibers have been demonstrated in the past as a polymeric combination capable of creating more spaces for cell migration over time while in cell culture because of this effect.<sup>45</sup> Although coaxial fiber porosity will remain consistent and not follow this trend, the overall structural integrity will be consistent, which may be a more favorable strategy for certain tissue engineering or wound healing applications.

Evidence of gelatin encapsulation of the coaxial fibers was verified using TEM and is shown in Figure 5. The inner diameter of the coaxial fibers was found to be  $187.9 \pm 46.68$

nm. The incorporation of GSNO into the core was also proven by observing the inside of ruptured fibers, where visible GSNO particles are seen. Although the inner gelatin core was properly incorporated into these fibers, there is some variation of the orientation of this inner component in terms of size and location. Having a wide range of inner core diameters can also explain the variation in NO release characteristics previously shown. Gelatin–GSNO cores that are more encapsulated by PCL will have a more delayed NO release, while fibers that have a larger inner core and thinner PCL sheath will be more likely to have increased NO release. Once this burst effect is finished, there is still a sustained and consistent NO release which is most likely attributed to the fibers containing the smaller core diameters.

### 3.4. Leaching of GSNO from Electrospun Scaffolds.

A direct relationship can be made between the amount of GSNO diffusion through the fibrous scaffolds and the NO release profiles shown previously. Typically, as a NO donor is brought out of a polymer matrix into solution, high bursts of NO will be initially seen and followed by a decay over a short time period. The blended fibers, in particular, had a characteristic burst release when placed under physiological conditions, so a high amount of leaching is to be anticipated. Although coaxial fibers should have a majority of the GSNO encapsulated, there will be instances of leaching as the inner core is degraded when placed in an aqueous environment. This NO donor leaching can be quantified to give insight into the longevity and release kinetics of a material.

Detection of the amount of GSNO leaching from the scaffolds was tested through UV–vis spectroscopy. Samples of both blended and coaxial fibers were weighed and tested in triplicate as absorbance was measured at 340 nm over the course of 24 h (Figure 6). By the end of the study,  $139.7 \pm 29.5 \mu\text{g}$  of GSNO per mg of the polymer was released from the blended scaffolds, while  $66.4 \pm 12.7 \mu\text{g}$  of GSNO per mg of the polymer was released from the coaxial scaffolds. Over this period, this indicates that approximately  $69.9 \pm 14.8\%$  of the GSNO is being leached from the blended fibers, while  $33.2 \pm 6.35\%$  is leached from the coaxial fibers. This observation was to be expected as the protective sheath from the coaxial fibers is able to slow the initial diffusion of GSNO to the surrounding environment, but it does not completely prevent it. Because of irregularities within the coaxial fiber structure, there is still some leaching present after 24 h. This could also be due to the high surface area of the fibrous scaffolds tested in combination with the high hydrophilicity of the gelatin–GSNO core as water is swelled within the fibers. Ruptured fibers during the electrospinning process would also assist in this leaching process, as this would propagate the dissolution of the core structure over time. However, the remaining GSNO within both fiber types explains the prolonged NO release seen after the first 24 h, which is typically not seen with most fabricated NO-incorporated fibrous matrices.

### 3.5. Antibacterial Characterization of Fabricated Fibers.

Infection is a major complication associated with tissue engineering, often prolonging the resolution of the healing process and leading to increased hospital stays and discomfort for the patient. One of the most common hospital-acquired infections (HAIs) is *S. aureus*. Materials capable of releasing NO have demonstrated effectiveness against a variety of bacteria by directly impacting DNA through deamination, denaturing important enzymes,

and lipid oxidation.<sup>60,61</sup> A major complication with tissue contacting biomaterials is when bacteria form biofilms, they encase themselves in a matrix consisting of a variety of proteins and polysaccharides, thus becoming resistant to the administration of antibiotics.<sup>62</sup> Due to the small size of NO, it is able to penetrate through this outer protective matrix and disrupt normal bacterial function. The use of NO is also unlikely to promote the production of antibiotic-resistant strains of bacteria because of their rapid action, short half-life, and nonspecific bacterial killing.

*In vitro* bacterial testing of both blended and coaxial GSNO fibers demonstrated to be effective in significantly reducing the amount of *S. aureus* adhesion over a 24 h testing period (Figure 7). There was very little difference in bacterial viability between the coaxial and blended GSNO fibers, displaying approximately a 3-log reduction in bacterial viability with both fiber types when compared to their respective controls. The preliminary prediction was that the leached GSNO and higher initial release from the blended fibers would play a larger role in the antibacterial properties. One hypothesis is that the sustained NO release profile plays a more important role compared to larger, burst releases of NO over a short period. As the inner core of the coaxial fibers is degraded when in an aqueous environment, a higher sustained NO release is seen over the course of the testing period, which was observed in the initial NO release trends. Over the course of the 24 h testing period, approximately 0.0675 and 0.0820  $\mu\text{mol}$  of NO per mg of the fiber was released from the blended GSNO and coaxial GSNO fibers, respectively. Although there was a substantial burst release initially from the blended fibers, most likely because of the increased leaching, the coaxial fibers were able to display similar antimicrobial capabilities and a higher total NO release. This again reinforces the claim that the initial NO-releasing kinetics from a material within the first 24 h is a key consideration when designing antibacterial biomaterials containing RSNOs.

### 3.6. Noncytotoxicity and Induction of Cell Adhesion, Proliferation, and Patterned Mammalian Cell Growth.

The diffusion of GSNO into its environment can prove to have cytotoxic effects on cells at certain levels. This is due the nitrosative and oxidative stress NO can demonstrate toward mammalian cells when at increased concentrations. Although GSNO itself is an endogenous molecule and is overall noncytotoxic at low levels, it is important to confirm there is high cell viability when exposed to the previously recorded leachate levels. Quantification of cell viability was carried out by first soaking the GSNO fibrous mats for 24 h in DMEM before transferring it to a culture of mouse fibroblast cells. Results showed that both types of fibers possessed no cytotoxic leachates, further emphasizing the capabilities of these fibrous scaffolds in biomedical applications. Figure 8 shows the relative cell viability compared to control fibrous scaffolds. This noncytotoxic trend is further proven from past studies that have demonstrated the safe application of materials that have incorporated GSNO.<sup>55,63</sup> This is a significant stride in the field of biomedical engineering as several antibacterial agents including antibiotics and silver nanoparticles can be cytotoxic to the mammalian cell system. This study therefore assures that NO-releasing fibrous mats containing GSNO in the blended or coaxial form are completely harmless to the mammalian cells at the concentration used in this study.

An observation of fibroblast attachment and proliferation was observed on the electrospun fibrous mats after 24 h of incubation. Cell nuclei were stained with DAPI, while cytoplasmic F-actin filaments were stained with phalloidin to observe the relative activity of the attached cells. There was a noticeable increase in attached fibroblast cell density on the fibrous scaffolds with NO release compared to their relative controls for the duration of the study (Figure 9). Without GSNO, comparison between the blended and coaxial fibers with no GSNO showed a slight increase in the blended composition when compared to the coaxial scaffolds. This is most likely due to the high favorability in cell attachment to gelatin, as it closely resembles the structure of native collagen. Both blended and coaxial fibers displayed an increase in fibroblast attachment when exposed to NO release, but a substantial increase was seen specifically in the coaxial GSNO fibers. This is most likely due to the difference in NO release kinetics between the two samples, as the burst release of NO is short lived within the blended sample, while the coaxial samples were able to maintain a relatively high and steady flux for the duration of the 24 h study. Although the role of NO in terms of fibroblast proliferation is still debated, this particular instance shows that steady elution of NO from a fibrous platform has a large impact on the attachment and proliferation behavior. These results give insight into designing NO-donating fibrous scaffolds that promote a high cell density, while simultaneously providing antimicrobial capabilities.

In the past, gelatin- and PCL-containing materials have shown excellent cell adhesion properties in separate studies.<sup>64,65</sup> Thus, the combination of both gelatin and PCL as the basal material in addition to NO release was expected to display a significant improvement. A closer examination on cell morphology along the fibrous scaffolds was also observed at higher magnification and is shown in Figure 10. Pseudopodia extension across the fibers was seen on all scaffolds, as electrospun matrices have been demonstrated in the past to direct cell migration.<sup>37</sup> The NO-releasing scaffolds displayed enlarged nuclei and greater cytoplasmic features compared to their relative controls, signifying an increase in fibroblast activity. For engineering tissue and wound healing scaffolds and dressings, this is an important quality to have as it increases the rate of collagen formation and remodeling of the ECM, ultimately leading to earlier healing resolution.

The delivery of NO from an exogenous RSNO source, *S*-nitroso-*N*-acetylpenicillamine (SNAP), directly into cell media has been investigated in the past to have limited to no proliferative effects on fibroblasts at certain concentrations.<sup>66,67</sup> However, the delivery of NO from a fibrous surface on which the fibroblasts are directly attached seems to invoke a much different response as shown from the previously mentioned results. This is the first time that this type of proliferation and attachment has been investigated from an electrospun fibrous structure using GSNO as the primary delivery mechanism. It is important to note that the leaching effect from the blended GSNO fibers still promoted a noticeable increase in viable attached cells to the scaffolds when compared to its relative control. However, more controlled and stable NO release kinetics as seen from the coaxial GSNO fibers demonstrate a more dramatic response from the fibroblasts in terms of overall activity and attachment.

## 4. CONCLUSIONS

Electrospun fibers consisting of gelatin and PCL were further modified with GSNO to form a NO-releasing scaffold with potential wound healing and tissue scaffolding properties. Two specific types of fibers were constructed where both polymer components along with GSNO are blended together and then electrospun or the gelatin-containing GSNO is coaxially electrospun with a PCL outer sheath. The NO-releasing characteristics were observed from both fiber types where blending the GSNO displayed a high burst effect followed by a low leveled off flux, while encapsulating the GSNO in coaxial fibers showed only a slight burst release, while demonstrating a steady increase in NO release as the inner core was degraded. SEM imaging of the fiber types displayed visible GSNO particles not completely encapsulated within the fibers in the blended GSNO combination, explaining the high leaching and burst release, while virtually no GSNO was present on the coaxial GSNO combination. Both fiber types were found to have nearly identical antimicrobial properties against *S. aureus* over a 24 h incubation period, indicating that burst and sustained NO release mechanics can express similar short-term bactericidal capabilities at the appropriate flux levels. Fibroblast adhesion and proliferation were also shown to be increased with the presence of NO release from the scaffolds when compared to their relative controls, with a substantial increase in cell count specifically on the coaxial GSNO fibers, which exhibited a much more sustained NO flux compared to the blended composition. This gives a new insight into GSNO's potential role in enhancing fibroblast activity with regard to the medium in which it is delivered. Because of this high affinity for cell attachment and proliferation, while simultaneously demonstrating significant antimicrobial properties, this proposed biodegradable combination of PCL and gelatin with incorporated GSNO has the potential for being applied as an effective wound dressing or cell scaffold for a multitude of tissue engineering applications.

## ACKNOWLEDGMENTS

This study was supported by the funds received from the National Institute of Health, USA grant, NIH R01HL134899, and DOD grant, K\_025\_2018.

## REFERENCES

- (1). Dhandayuthapani B; Yoshida Y; Maekawa T; Kumar DS Polymeric Scaffolds in Tissue Engineering Application: A Review. *Int. J. Polym. Sci* 2011, 2011, 290602.
- (2). Xu C; Inai R; Kotaki M; Ramakrishna S Aligned biodegradable nanofibrous structure: a potential scaffold for blood vessel engineering. *Biomaterials* 2004, 25, 877–886. [PubMed: 14609676]
- (3). Lee SJ; Yoo JJ; Lim GJ; Atala A; Stitzel J In vitro evaluation of electrospun nanofiber scaffolds for vascular graft application. *J. Biomed. Mater. Res., Part A* 2007, 83A, 999–1008.
- (4). Yusof NLBM; Wee A; Lim LY; Khor E Flexible chitin films as potential wound-dressing materials: Wound model studies. *J. Biomed. Mater. Res., Part A* 2003, 66, 224–232.
- (5). Sui G; Yang X; Mei F; Hu X; Chen G; Deng X; Ryu S Poly-L-lactic acid/hydroxyapatite hybrid membrane for bone tissue regeneration. *J. Biomed. Mater. Res., Part A* 2007, 82, 445–454.
- (6). Hay ED Collagen and other matrix glycoproteins in embryogenesis. In *Cell Biology of Extracellular Matrix*; Springer, 1991; pp 419–462.
- (7). Lai H-J; Kuan C-H; Wu H-C; Tsai J-C; Chen T-M; Hsieh D-J; Wang T-W Tailored design of electrospun composite nanofibers with staged release of multiple angiogenic growth factors for chronic wound healing. *Acta Biomater* 2014, 10, 4156–4166. [PubMed: 24814882]

- (8). Xie Z; Paras CB; Weng H; Punnakitikashem P; Su L-C; Vu K; Tang L; Yang J; Nguyen KT Dual growth factor releasing multi-functional nanofibers for wound healing. *Acta Biomater* 2013, 9, 9351–9359. [PubMed: 23917148]
- (9). Sohrabi A; Shaibani PM; Etayash H; Kaur K; Thundat T Sustained drug release and antibacterial activity of ampicillin incorporated poly (methyl methacrylate)–nylon6 core/shell nanofibers. *Polymer* 2013, 54, 2699–2705.
- (10). Xie J; Wang C-H Electrospun micro-and nanofibers for sustained delivery of paclitaxel to treat C6 glioma in vitro. *Pharm. Res* 2006, 23, 1817. [PubMed: 16841195]
- (11). Witte M; Thornton F; Kiyama T; Tantry U; Barbul A Nitric oxide enhances wound collagen deposition in diabetic rats. *Surgical Forum-Chicago; American College of Surgeons*, 1997; pp 665–666.
- (12). Shabani M; Pulfer SK; Bulgrin JP; Smith DJ Enhancement of wound repair with a topically applied nitric oxide-releasing polymer. *Wound Repair Regen* 1996, 4, 353–362. [PubMed: 17177732]
- (13). Martinez LR; Han G; Chacko M; Mihu MR; Jacobson M; Gialanella P; Friedman AJ; Nosanchuk JD; Friedman JM Antimicrobial and healing efficacy of sustained release nitric oxide nanoparticles against *Staphylococcus aureus* skin infection. *J. Invest. Dermatol* 2009, 129, 2463–2469. [PubMed: 19387479]
- (14). Reighard KP; Schoenfisch MH Antibacterial action of nitric oxide-releasing chitosan oligosaccharides against *Pseudomonas aeruginosa* under aerobic and anaerobic conditions. *Antimicrob. Agents Chemother* 2015, 59, 6506. [PubMed: 26239983]
- (15). Hetrick EM; Shin JH; Paul HS; Schoenfisch MH Anti-biofilm efficacy of nitric oxide-releasing silica nanoparticles. *Biomaterials* 2009, 30, 2782–2789. [PubMed: 19233464]
- (16). Pant J; Gao J; Goudie MJ; Hopkins SP; Locklin J; Handa H A multi-defense strategy: Enhancing bactericidal activity of a medical grade polymer with a nitric oxide donor and surface-immobilized quaternary ammonium compound. *Acta Biomater* 2017, 58, 421–431. [PubMed: 28579540]
- (17). Pant J; Goudie MJ; Chaji SM; Johnson BW; Handa H Nitric oxide releasing vascular catheters for eradicating bacterial infection. *J. Biomed. Mater. Res., Part B* 2018, 106, 2849–2857.
- (18). Donlan RM; Costerton JW Biofilms: survival mechanisms of clinically relevant microorganisms. *Clin. Microbiol. Rev* 2002, 15, 167–193. [PubMed: 11932229]
- (19). Barraud N; Schleheck D; Klebensberger J; Webb JS; Hassett DJ; Rice SA; Kjelleberg S Nitric oxide signaling in *Pseudomonas aeruginosa* biofilms mediates phosphodiesterase activity, decreased cyclic di-GMP levels, and enhanced dispersal. *J. Bacteriol* 2009, 191, 7333–7342. [PubMed: 19801410]
- (20). Howlin RP; Cathie K; Hall-Stoodley L; Cornelius V; Duignan C; Allan RN; Fernandez BO; Barraud N; Bruce KD; Jefferies J; Kelso M; Kjelleberg S; Rice SA; Rogers GB; Pink S; Smith C; Sukhtankar PS; Salib R; Legg J; Carroll M; Daniels T; Feelisch M; Stoodley P; Clarke SC; Connett G; Faust SN; Webb JS Low-dose nitric oxide as targeted anti-biofilm adjunctive therapy to treat chronic *Pseudomonas aeruginosa* infection in cystic fibrosis. *Mol. Ther* 2017, 25, 2104–2116. [PubMed: 28750737]
- (21). Wang Y; Chen S; Pan Y; Gao J; Tang D; Kong D; Wang S Rapid in situ endothelialization of a small diameter vascular graft with catalytic nitric oxide generation and promoted endothelial cell adhesion. *J. Mater. Chem. B* 2015, 3, 9212–9222. [PubMed: 32263136]
- (22). Wang Z; Lu Y; Qin K; Wu Y; Tian Y; Wang J; Zhang J; Hou J; Cui Y; Wang K; Shen J; Xu Q; Kong D; Zhao Q Enzyme-functionalized vascular grafts catalyze in-situ release of nitric oxide from exogenous NO prodrug. *J. Controlled Release* 2015, 210, 179–188.
- (23). Morbidelli L; Chang CH; Douglas JG; Granger HJ; Ledda F; Ziche M Nitric oxide mediates mitogenic effect of VEGF on coronary venular endothelium. *Am. J. Physiol.: Heart Circ. Physiol* 1996, 270, H411–H415.
- (24). Coneski PN; Nash JA; Schoenfisch MH Nitric oxide-releasing electrospun polymer microfibers. *ACS Appl. Mater. Interfaces* 2011, 3, 426–432. [PubMed: 21250642]

- (25). Koh A; Carpenter AW; Slomberg DL; Schoenfisch MH Nitric oxide-releasing silica nanoparticle-doped polyurethane electrospun fibers. *ACS Appl. Mater. Interfaces* 2013, 5, 7956–7964. [PubMed: 23915047]
- (26). Worley BV; Soto RJ; Kinsley PC; Schoenfisch MH Active Release of Nitric Oxide-Releasing Dendrimers from Electrospun Polyurethane Fibers. *ACS Biomater. Sci. Eng* 2016, 2, 426–437. [PubMed: 32309632]
- (27). Hart TW Some observations concerning the S-nitroso and S-phenylsulphonyl derivatives of L-cysteine and glutathione. *Tetrahedron Lett* 1985, 26, 2013–2016.
- (28). Zhang Y; Ouyang H; Lim CT; Ramakrishna S; Huang Z-M Electrospinning of gelatin fibers and gelatin/PCL composite fibrous scaffolds. *J. Biomed. Mater. Res., Part B* 2005, 72, 156–165.
- (29). Pant J; Goudie MJ; Hopkins SP; Brisbois EJ; Handa H Tunable Nitric Oxide Release from S-Nitroso-N-acetylpenicillamine via Catalytic Copper Nanoparticles for Biomedical Applications. *ACS Appl. Mater. Interfaces* 2017, 9, 15254–15264. [PubMed: 28409633]
- (30). Pant J; Gao J; Goudie MJ; Hopkins S; Locklin J; Handa H A Multi-defense Strategy: Enhancing Bactericidal Activity of a Medical Grade Polymer with a Nitric Oxide Donor and Surface-immobilized Quaternary Ammonium Compound. *Acta Biomater* 2017, 58, 421. [PubMed: 28579540]
- (31). Li C; Vepari C; Jin H-J; Kim HJ; Kaplan DL Electrospun silk-BMP-2 scaffolds for bone tissue engineering. *Biomaterials* 2006, 27, 3115–3124. [PubMed: 16458961]
- (32). Shin M; Yoshimoto H; Vacanti JP In vivo bone tissue engineering using mesenchymal stem cells on a novel electrospun nanofibrous scaffold. *Tissue Eng* 2004, 10, 33–41. [PubMed: 15009928]
- (33). Hasan A; Memic A; Annabi N; Hossain M; Paul A; Dokmeci MR; Dehghani F; Khademhosseini A Electrospun scaffolds for tissue engineering of vascular grafts. *Acta Biomater* 2014, 10, 11–25. [PubMed: 23973391]
- (34). Hashi CK; Zhu Y; Yang G-Y; Young WL; Hsiao BS; Wang K; Chu B; Li S Antithrombogenic property of bone marrow mesenchymal stem cells in nanofibrous vascular grafts. *Proc. Natl. Acad. Sci. U.S.A* 2007, 104, 11915–11920. [PubMed: 17615237]
- (35). Rho KS; Jeong L; Lee G; Seo B-M; Park YJ; Hong S-D; Roh S; Cho JJ; Park WH; Min B-M Electrospinning of collagen nanofibers: effects on the behavior of normal human keratinocytes and early-stage wound healing. *Biomaterials* 2006, 27, 1452–1461. [PubMed: 16143390]
- (36). Choi JS; Leong KW; Yoo HS In vivo wound healing of diabetic ulcers using electrospun nanofibers immobilized with human epidermal growth factor (EGF). *Biomaterials* 2008, 29, 587–596. [PubMed: 17997153]
- (37). Schnell E; Klinkhammer K; Balzer S; Brook G; Klee D; Dalton P; Mey J Guidance of glial cell migration and axonal growth on electrospun nanofibers of poly- $\epsilon$ -caprolactone and a collagen/poly- $\epsilon$ -caprolactone blend. *Biomaterials* 2007, 28, 3012–3025. [PubMed: 17408736]
- (38). Glass-Brudzinski J; Perizzolo D; Brunette D Effects of substratum surface topography on the organization of cells and collagen fibers in collagen gel cultures. *J. Biomed. Mater. Res* 2002, 61, 608–618. [PubMed: 12115451]
- (39). Venugopal J; Ramakrishna S Biocompatible nanofiber matrices for the engineering of a dermal substitute for skin regeneration. *Tissue Eng* 2005, 11, 847–854. [PubMed: 15998224]
- (40). Papapetropoulos A; García-Cardena G; Madri JA; Sessa WC Nitric oxide production contributes to the angiogenic properties of vascular endothelial growth factor in human endothelial cells. *J. Clin. Invest* 1997, 100, 3131. [PubMed: 9399960]
- (41). Schairer DO; Chouake JS; Nosanchuk JD; Friedman AJ The potential of nitric oxide releasing therapies as antimicrobial agents. *Virulence* 2012, 3, 271–279. [PubMed: 22546899]
- (42). Hetrick EM; Prichard HL; Klitzman B; Schoenfisch MH Reduced foreign body response at nitric oxide-releasing subcutaneous implants. *Biomaterials* 2007, 28, 4571–4580. [PubMed: 17681598]
- (43). Handa H; Brisbois EJ; Major TC; Refahiyat L; Amoako KA; Annich GM; Bartlett RH; Meyerhoff ME In vitro and in vivo study of sustained nitric oxide release coating using diazeniumdiolate-doped poly (vinyl chloride) matrix with poly (lactide-co-glycolide) additive. *J. Mater. Chem. B* 2013, 1, 3578–3587. [PubMed: 23914297]

- (44). Ghasemi-Mobarakeh L; Prabhakaran MP; Morshed M; Nasr-Esfahani M-H; Ramakrishna S Electrospun poly ( $\epsilon$ -caprolactone)/gelatin nanofibrous scaffolds for nerve tissue engineering. *Biomaterials* 2008, 29, 4532–4539. [PubMed: 18757094]
- (45). Chong E; Phan T; Lim I; Zhang Y; Bay B; Ramakrishna S; Lim C Evaluation of electrospun PCL/gelatin nanofibrous scaffold for wound healing and layered dermal reconstitution. *Acta Biomater* 2007, 3, 321–330. [PubMed: 17321811]
- (46). Binulal NS; Natarajan A; Menon D; Bhaskaran VK; Mony U; Nair SV PCL–gelatin composite nanofibers electrospun using diluted acetic acid–ethyl acetate solvent system for stem cell-based bone tissue engineering. *J. Biomater. Sci., Polym. Ed* 2014, 25, 325–340. [PubMed: 24274102]
- (47). Kim SE; Heo DN; Lee JB; Kim JR; Park SH; Jeon SH; Kwon IK Electrospun gelatin/polyurethane blended nanofibers for wound healing. *Biomed. Mater* 2009, 4, 044106. [PubMed: 19671952]
- (48). Chen F; Li X; Mo X; He C; Wang H; Ikada Y Electrospun chitosan-P (LLA-CL) nanofibers for biomimetic extracellular matrix. *J. Biomater. Sci., Polym. Ed* 2008, 19, 677–691. [PubMed: 18419945]
- (49). Kuihua Z; Chunyang W; Cunyi F; Xiumei M Aligned SF/P (LLA-CL)-blended nanofibers encapsulating nerve growth factor for peripheral nerve regeneration. *J. Biomed. Mater. Res., Part A* 2014, 102, 2680–2691.
- (50). Sell SA; Wolfe PS; Garg K; McCool JM; Rodriguez IA; Bowlin GL The use of natural polymers in tissue engineering: a focus on electrospun extracellular matrix analogues. *Polymers* 2010, 2, 522–553.
- (51). Zhang Y; Huang Z-M; Xu X; Lim CT; Ramakrishna S Preparation of core– shell structured PCL-r-gelatin bi-component nanofibers by coaxial electrospinning. *Chem. Mater* 2004, 16, 3406–3409.
- (52). Zhang Y; Su B; Venugopal J; Ramakrishna S; Lim C Biomimetic and bioactive nanofibrous scaffolds from electrospun composite nanofibers. *Int. J. Nanomed* 2007, 2, 623.
- (53). Hu X; Liu S; Zhou G; Huang Y; Xie Z; Jing X Electrospinning of polymeric nanofibers for drug delivery applications. *J. Controlled Release* 2014, 185, 12–21.
- (54). Khan M; Dhammu T; Matsuda F; Baarine M; Dhindsa T; Singh I; Singh A Promoting endothelial function by S-nitrosoglutathione through the HIF-1 $\alpha$ /VEGF pathway stimulates neuro-repair and functional recovery following experimental stroke in rats. *Drug Des., Dev. Ther* 2015, 9, 2233–2247.
- (55). Seabra AB; da Rocha LL; Eberlin MN; de Oliveira MG Solid films of blended poly (vinyl alcohol)/poly (vinyl pyrrolidone) for topical S-nitrosoglutathione and nitric oxide release. *J. Pharm. Sci* 2005, 94, 994–1003. [PubMed: 15793801]
- (56). Georgii JL; Amadeu TP; Seabra AB; de Oliveira MG; Monte-Alto-Costa A Topical S-nitrosoglutathione-releasing hydrogel improves healing of rat ischaemic wounds. *J. Tissue Eng. Regener. Med* 2011, 5, 612–619.
- (57). Amadeu TP; Seabra AB; De Oliveira MG; Costa AM S-nitrosoglutathione-containing hydrogel accelerates rat cutaneous wound repair. *J. Eur. Acad. Dermatol. Venereol* 2007, 21, 629–637. [PubMed: 17447976]
- (58). Li W-J; Laurencin CT; Cateson EJ; Tuan RS; Ko FK Electrospun nanofibrous structure: a novel scaffold for tissue engineering. *J. Biomed. Mater. Res., Part A* 2002, 60, 613–621.
- (59). Leung V; Ko F Biomedical applications of nanofibers. *Polym. Adv. Technol* 2011, 22, 350–365.
- (60). De Groote MA; Fang FC NO inhibitions: antimicrobial properties of nitric oxide. *Clin. Infect. Dis* 1995, 21, S162–S165. [PubMed: 8845445]
- (61). Carpenter AW; Schoenfish MH Nitric oxide release: Part II. Therapeutic applications. *Chem. Soc. Rev* 2012, 41, 3742–3752. [PubMed: 22362384]
- (62). Mah T-FC; O’Toole GA Mechanisms of biofilm resistance to antimicrobial agents. *Trends Microbiol* 2001, 9, 34–39. [PubMed: 11166241]
- (63). Parent M; Boudier A; Fries I; Gostyska A; Rychter M; Lulek J; Leroy P; Gaucher C Nitric oxide-eluting scaffolds and their interaction with smooth muscle cells in vitro. *J. Biomed. Mater. Res., Part A* 2015, 103, 3303–3311.



- (64). Venugopal JR; Zhang Y; Ramakrishna S In vitro culture of human dermal fibroblasts on electrospun polycaprolactone collagen nanofibrous membrane. *Artif. Organs* 2006, 30, 440–446. [PubMed: 16734595]
- (65). Sisson K; Zhang C; Farach-Carson MC; Chase DB; Rabolt JF Evaluation of cross-linking methods for electrospun gelatin on cell growth and viability. *Biomacromolecules* 2009, 10, 1675–1680. [PubMed: 19456101]
- (66). Zhu H; Ka B; Murad F Nitric oxide accelerates the recovery from burn wounds. *World J. Surg* 2007, 31, 624–631. [PubMed: 17308846]
- (67). Villalobo A REVIEW ARTICLE: Nitric oxide and cell proliferation. *FEBS J* 2006, 273, 2329–2344. [PubMed: 16704409]

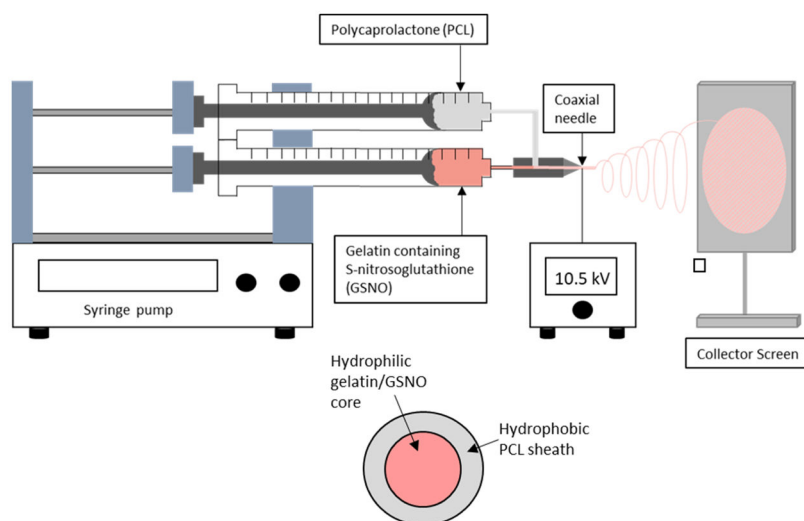


**Figure 1.** Electrospinning setup for the fabrication of core-shell GSNO-containing fibers. The inner core contains 10 wt % gelatin in HFIP with 20 wt % GSNO thoroughly mixed in. The outer sheath contains 10 wt % PCL in HFIP.

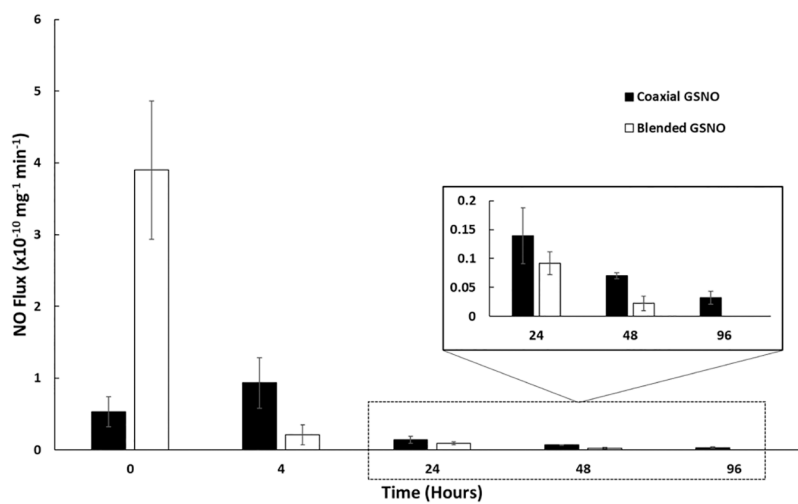


**Figure 2.** Measured NO flux from electrospun dressings over the course of 96 h for both coaxial and blended incorporated GSNO samples.

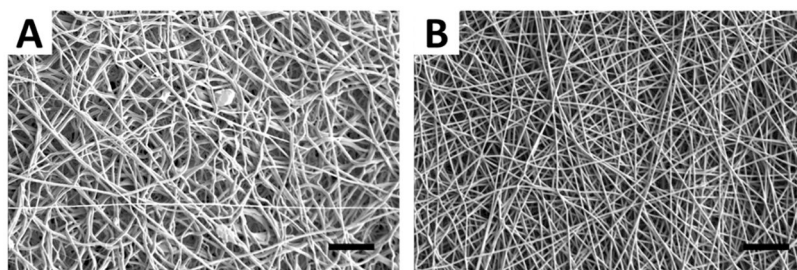


**Figure 3.** SEM images of (A) blended GSNO and (B) coaxial GSNO fibers. Scale bars = 20  $\mu\text{m}$ .

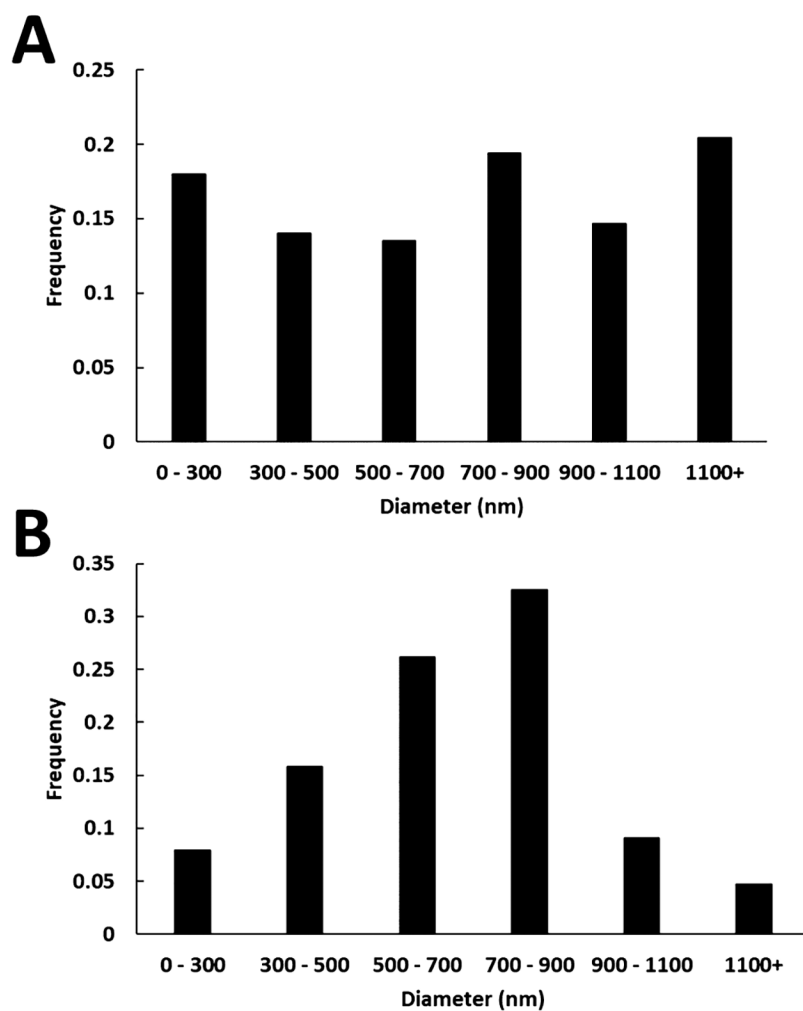


**Figure 4.** Diameter distribution of (A) blended GSNO fibers and (B) coaxial GSNO fibers. Fiber analysis was carried out using ImageJ software.

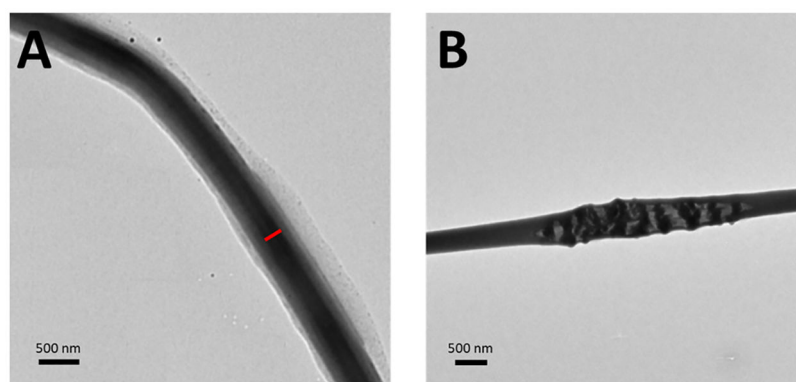


**Figure 5.** TEM images of coaxial fibers. (A) Red bar indicates the inner core diameter within the fibrous structure (left). (B) Proof of encapsulation of GSNO particles is shown within a ruptured coaxial fiber.

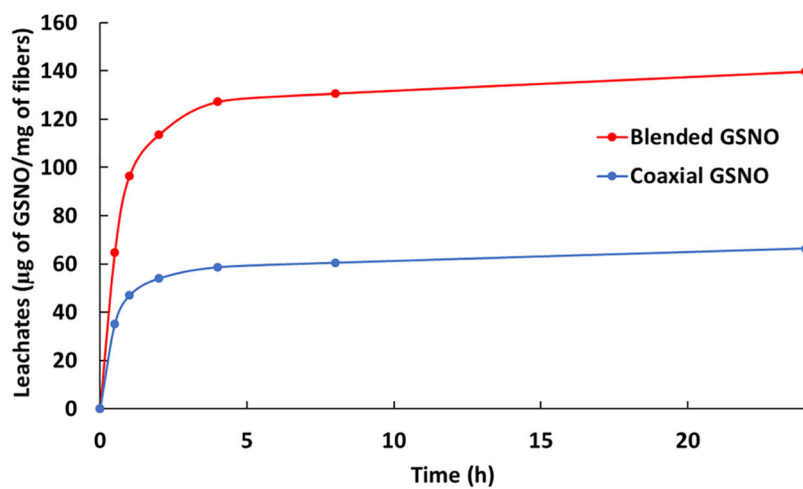


**Figure 6.** Cumulative leaching from blended and coaxial GSNO fibers over the course of 24 h when submerged in PBS at 37 °C.

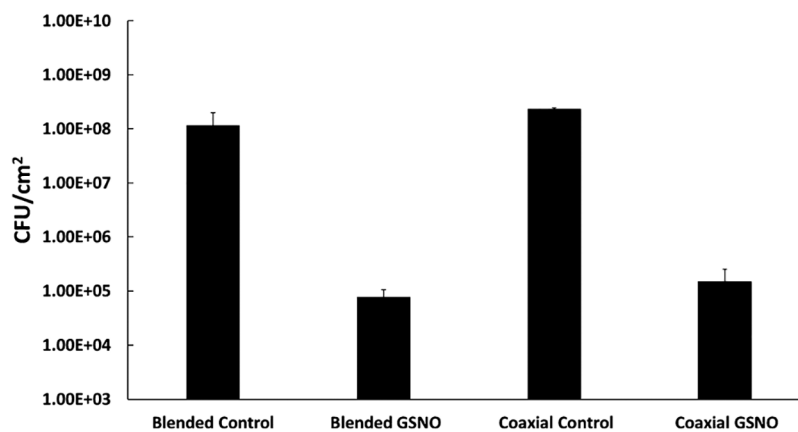


**Figure 7.** Bacterial viability study of fabricated fibrous materials against *S. aureus* after 24 h. A significant reduction in viability was seen between both NO-releasing fibrous scaffolds with respect to their relative controls ( $P < 0.05$ ).



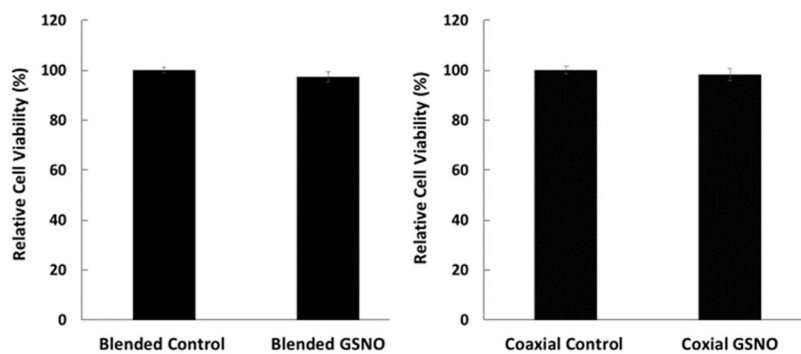


**Figure 8.** Cell cytotoxicity of leachable components from electrospun fibrous materials to the mouse fibroblast 3T3 cell line.

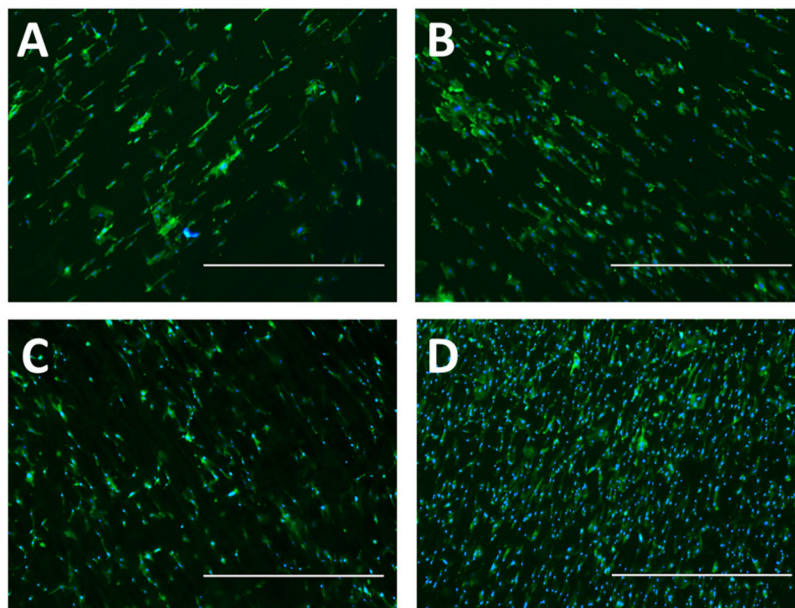


**Figure 9.** Cell nuclei (DAPI, blue)- and F-actin (phalloidin, green)-stained mouse fibroblasts cultured for 24 h on (A) blended fibers, (B) blended GSNO fibers, (C) coaxial fibers, and (D) coaxial GSNO fibers. Fibers were electrospun onto glass coverslips. 40× magnification; scale bars represent 1000  $\mu\text{m}$ .

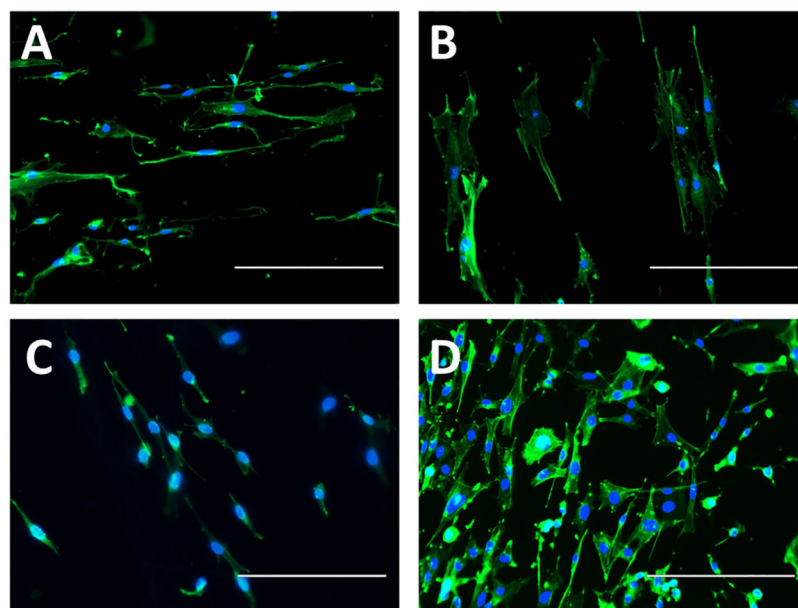


**Figure 10.** Cell nuclei (DAPI, blue)- and F-actin (phalloidin, green)-stained mouse fibroblasts cultured for 24 h on (A) blended fibers, (B) blended GSNO fibers, (C) coaxial fibers, and (D) coaxial GSNO fibers. Fibers were electrospun onto glass coverslips. 200× magnification; scale bars represent 200  $\mu\text{m}$ .